AGRICULTURAL PLATFORM EQUIPPED WITH A HYDROSTATIC TRANSMISSION CAPABLE OF CONTINUOUSLY ADJUSTABLE TRAVEL VELOCITY AND NON-LINEAR DISTURBANCE COMPENSATION CAPABILITIES
/
PLATFORMĂ AGRICOLĂ DOTATĂ CU O TRANSMISIE HIDROSTATICĂ CAPABILĂ SĂ REALIZEZE VITEZE DE DEPLASARE CONTINUU VARIABILE ȘI CAPABILITĂȚI DE COMPENSARE A PERTURBAȚIILOR NELINIARE

Alexandru-Polifron CHIRIȚĂ*1),2) [1]; Cristian PAVEL2)
1) INOE 2000 - Subsidiary Hydraulics and Pneumatics Research Institute / Romania;
2) Faculty of Mechanical Engineering and Robotics in Construction, Technical University of Civil Engineering Bucharest / Romania
** E-mail: chirita.ihp@fluidas.ro*

DOI: https://doi.org/10.35633/inmateh-69-40

Keywords: *precision agriculture platform, continuously variable velocity, feedforward*

ABSTRACT

Both in the case of precision agriculture and in the case of some agricultural works, in which the technological process is dependent on the velocity of displacement of the platform carrying the agricultural equipment, it is necessary to precisely adjust or even continuously adjust the velocity of displacement. This article presents the capabilities of continuously regulating the travel velocity of an agricultural platform equipped with a hydrostatic transmission and a PID controller with feedback, feedforward, as well as nonlinear disturbance compensation capabilities; such a platform can be fitted with various agricultural equipment.

REZUMAT

Atât în cazul agriculturii de precizie, cât și în cazul unor lucrări agricole în care procesul tehnologic este dependent de viteza de deplasare a platformei purtătoare de echipamente agricole, este necesară reglarea cu precizie sau chiar reglarea continuă a vitezei de deplasare. Acest articol prezintă capabilitățile de reglare continuă a vitezei de deplasare a unei platforme agricole dotată cu o transmisie hidrostatică și un regulator PID cu feedback, feedforward, precum și capabilități de compensare a perturbațiilor neliniare, platformă ce poate fi dotată cu diverse echipamente agricole.

INTRODUCTION

Studies on the mechanics of agricultural machinery, such as tractors, are getting better and better as agricultural modernization and intelligence levels continue to advance *(Cheng and Lu, 2021; Balafoutis et al., 2017)*. Precision agriculture is the use of information and communications technologies to control the spatial and temporal variation in the fields related to the soil, atmosphere, and plants *(Zhang, 2015)*. Agricultural vehicles frequently use hydrostatic transmissions, which are continuously variable transmissions that vary steplessly across an infinite range of effective transmission ratios *(Guo and Hu, 2014; Warring, 2014)*. The power given to the driving wheels from the engine, the tire pressure and the state of the field's terrain all affect the travel velocity, so in order to carry out the whole process in an optimized manner and prevent possible damage to the crops a precise continuously performed velocity control is needed. It is challenging to develop an appropriate mathematical model for this process since it is a complicated, multi-variable, nonlinear, time-varying system.

In their study, *Li et al. (2021)* aimed to design a hydraulic drive system for an orchard conveyor that addresses the issues and complexity of traditional transmission systems. The new system they propose allows for quick reversal, stepless speed regulation, and instantaneous braking. To test the feasibility of this system, they used simulations to mimic the operation of an orchard conveyor under different load states. Another study - *(Hu et al., 2021)* - has proposed a technical solution of a fully hydraulic chassis drive system for tractors in hilly and mountainous areas in order to address the adaptation problem of traditional tractors in these areas. The results show that the motor performance must meet demanding requirements in terms of working pressure, output torque, and output velocity. *Cheng and Lu, (2022),* have developed a hydro-mechanical continuously variable transmission with optimized speed-regulating characteristics for use in precision agriculture with tractors.

---

[1] *Alexandru-Polifron Chiriță, PhD. Stud. Eng.; Cristian Pavel, Prof. PhD. Eng.*

The transmission uses eight gear pairs, two planetary rows, three wet clutches, a variable-pump and a constant speed motor. *Guo et al., (2013)* developed a GPS-based intelligent operation control system for rice transplanters in order to regulate travel speed in accordance with the prescribed map.

MATERIALS AND METHODS

Since the velocity of displacement of the platforms carrying various agricultural technological equipment is in some cases dependent on the technological process, with the help of the AMESim (**A**dvanced **M**odeling **E**nvironment for performing **Sim**ulations of engineering systems), the dynamic parameters of these platforms have been optimized. Because the technological processes in the agricultural field do not require travel speeds higher than 12 km/h and because it is necessary to continuously adjust the travel velocity to improve productivity or because the technological process requires it, it has been chosen for the agricultural platform to be equipped with a closed-loop hydrostatic transmission, with primary control *(Tecușan and Ionescu, 1982)*.

Fig. 1 shows the simulation network of the agricultural platform equipped with a closed-loop primary regulation hydrostatic transmission. The simulation model shown in Fig. 1 comprises a hydrostatic transmission, a prime mover that can be a thermal engine or an electric one powered by batteries and the agricultural platform with all-wheel drive. The platform tows technological equipment that performs a technological operation simultaneously with the measurement of the travel speed; that travel speed is transmitted to the comparator element of the PID (**P**roportional **I**ntegral **D**erivative) controller with feedback, feedforward and capabilities for compensation of non-linear phenomena.

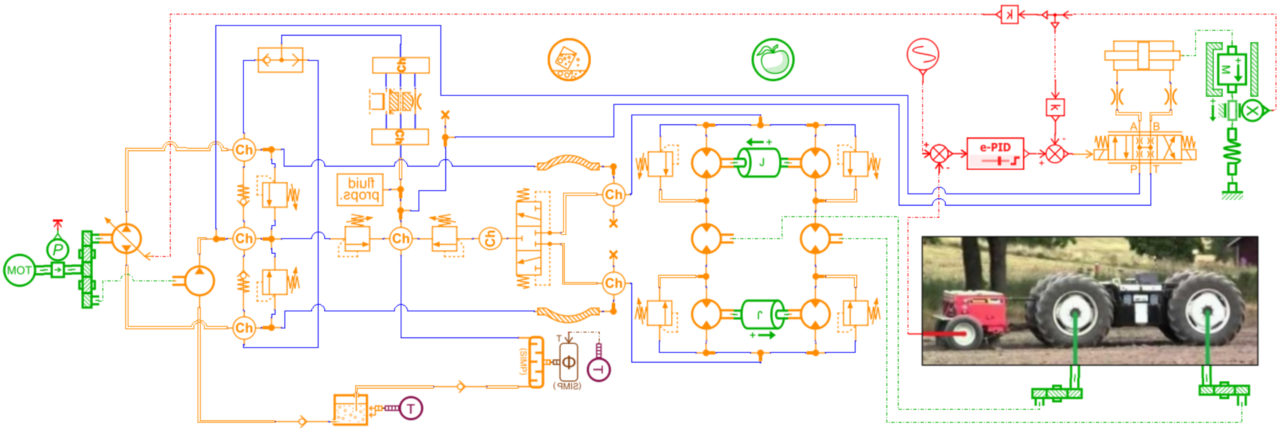

Fig. 1 - The simulation network of the agricultural platform

The hydrostatic transmission is composed of a servo-pump whose main pump has a displacement of 210 cm^3/rev; a compensation pump with a displacement of 32 cm^3/rev; the relief valves acting as safety valves in the closed-loop circuit are set at 350 bar, and the compensation pump relief valve is set at 25 bar; the check valves open at 0.5 bar. The simulation model also takes into account the volumetric losses of the transmission; they are modeled in detail, through three interstices of different shapes and sections because the results should be as close to reality as possible. Also, in the structure of the servo-pump there is the servo-mechanism for regulating the pump displacement; the numerical simulation model of that servo-mechanism has been experimentally validated by *Chiriță and Pavel, (2022)*. As part of the hydrostatic transmission structure, there are also two hydrostatic motors with a displacement of 300 cm^3/rev and a maximum pressure of 450 bar. They are connected to the two axles of the agricultural platform that have the transmission ratio i = 4; since the load on the two motor axles of the platform is 60% (rear) and 40% (front), it was necessary to use flow rate dividers, which divide the flow rate of the servo-pump equally, regardless of the load (torque or pressure); the two flow dividers fulfil the role of a lockable differential; each of these is composed of two hydraulic motors with gears that have a displacement of 52.5 cm^3/rev and two pressure relief valves that have the role of bypassing the motors if the pressure exceeds 300 bar. In close proximity to the hydrostatic motors, there is also connected a flushing valve whose relief valve is set at 20 bar. The numerical simulation model also includes a heat exchanger with a volume of 10 L, which has the role of maintaining the hydraulic fluid at an optimal temperature and viscosity, together with a hydraulic fluid tank model with a volume of 35 L and variable height of fluid level.

All hydraulic components of the transmission, those coloured in orange in the simulation network, take into account the effects of temperature on the hydraulic fluid and hydraulic components.

Fig. 2 presents the parameters of the PID controller for the case of its manual tuning and the linearization of the physical process required for automatic tuning (on the gain curve); in the same figure one can notice that the physical process corresponds to one of a 2nd order system with a 99.5% match and a natural frequency of 4.5 Hz.

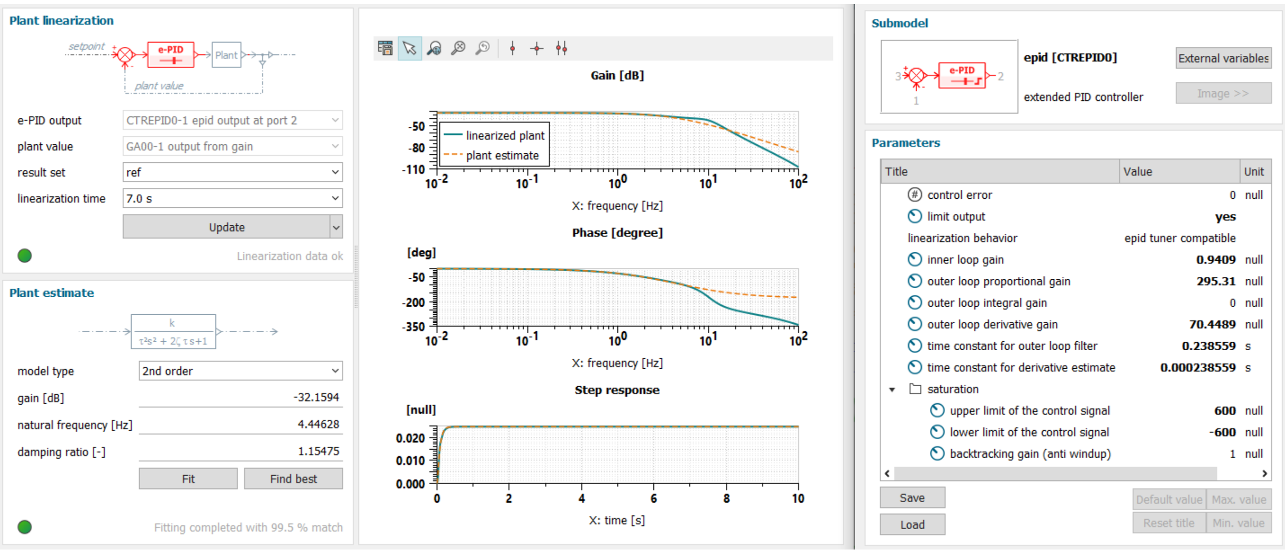

e-PID output: CTREPID0-1 epid output at port 2
plant value: GA00-1 output from gain
result set: ref
linearization time: 7.0 s
Linearization data ok

model type: 2nd order
gain [dB]: -32.1594
natural frequency [Hz]: 4.44628
damping ratio [-]: 1.15475
Fitting completed with 99.5 % match

epid [CTREPID0]
extended PID controller

Title	Value	Unit
control error	0	null
limit output	**yes**	
linearization behavior	epid tuner compatible	
inner loop gain	**0.9409**	null
outer loop proportional gain	**295.31**	null
outer loop integral gain	0	null
outer loop derivative gain	**70.4489**	null
time constant for outer loop filter	**0.238559**	s
time constant for derivative estimate	**0.000238559**	s
saturation		
upper limit of the control signal	**600**	null
lower limit of the control signal	**-600**	null
backtracking gain (anti windup)	1	null

Fig. 2 - Plant linearization for automatic PID controller tuning and controller parameters for manual tuning

Because closed-loop hydrostatic transmissions whose parameters are not well optimized suffer from overheating and the servo-pumps equipping them face premature wearing out due to the cavitation that occurs on the suction port of the pump, an advanced fluid model that takes into account the influence of temperature and advanced laws for cavitation has been used. The fluid parameters can be consulted in Fig. 3 below.

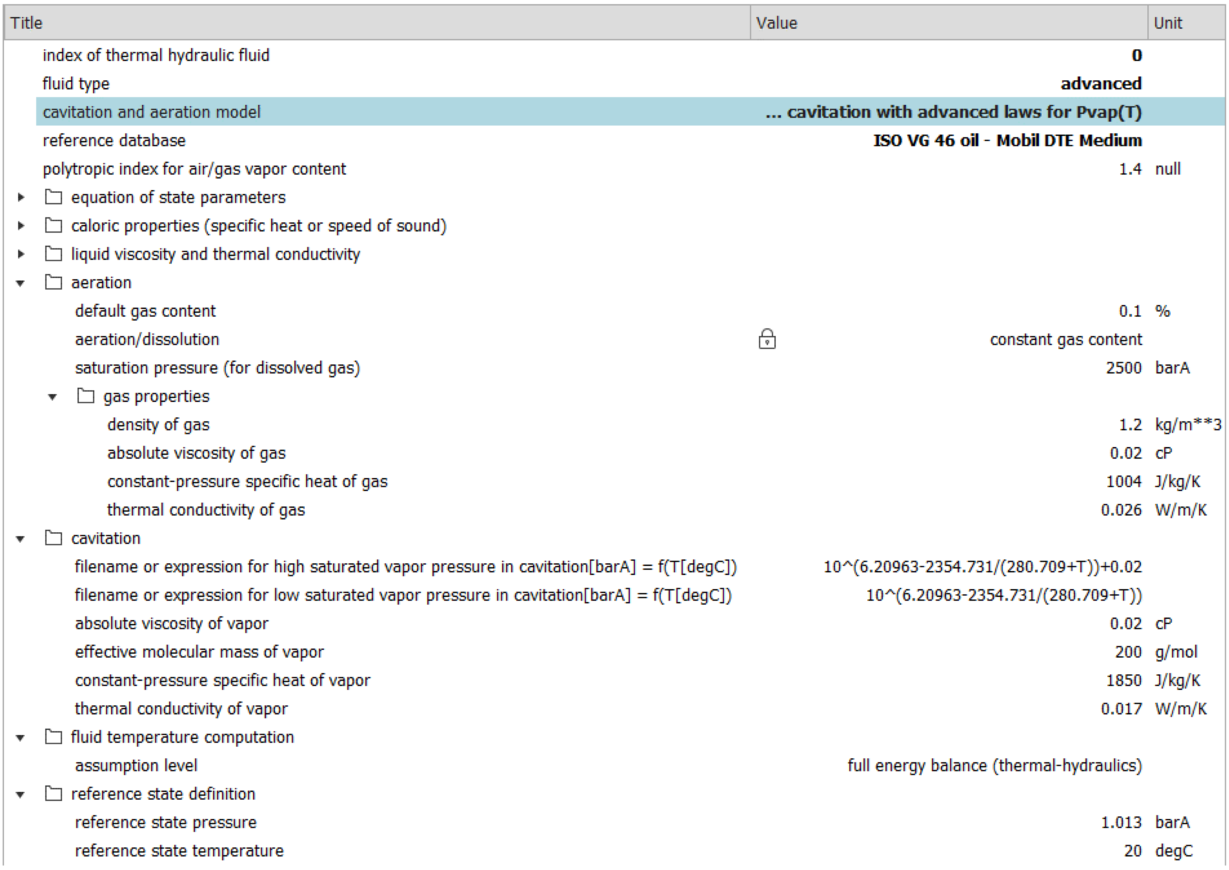

Title	Value	Unit
index of thermal hydraulic fluid	**0**	
fluid type	**advanced**	
cavitation and aeration model	**... cavitation with advanced laws for Pvap(T)**	
reference database	**ISO VG 46 oil - Mobil DTE Medium**	
polytropic index for air/gas vapor content	1.4	null
equation of state parameters		
caloric properties (specific heat or speed of sound)		
liquid viscosity and thermal conductivity		
aeration		
default gas content	0.1	%
aeration/dissolution	constant gas content	
saturation pressure (for dissolved gas)	2500	barA
gas properties		
density of gas	1.2	kg/m**3
absolute viscosity of gas	0.02	cP
constant-pressure specific heat of gas	1004	J/kg/K
thermal conductivity of gas	0.026	W/m/K
cavitation		
filename or expression for high saturated vapor pressure in cavitation[barA] = f(T[degC])	10^(6.20963-2354.731/(280.709+T))+0.02	
filename or expression for low saturated vapor pressure in cavitation[barA] = f(T[degC])	10^(6.20963-2354.731/(280.709+T))	
absolute viscosity of vapor	0.02	cP
effective molecular mass of vapor	200	g/mol
constant-pressure specific heat of vapor	1850	J/kg/K
thermal conductivity of vapor	0.017	W/m/K
fluid temperature computation		
assumption level	full energy balance (thermal-hydraulics)	
reference state definition		
reference state pressure	1.013	barA
reference state temperature	20	degC

Fig. 3 - Parameters of the advanced hydraulic fluid model

RESULTS

Running the numerical simulation model for a 10-second period, in which the agricultural platform moves on rough terrain with a 45% slope (the first 5 seconds for ascending the slope with variable velocity and the other 5 seconds for descending the slope, also with variable velocity), results in the graphs that will be presented below.

The speed of the shaft of the servo-pump together with the time-variation of the resistant torque to the shaft of the same pump and the power consumed by it can be seen in Fig. 4. In the same figure one can see that the speed is constant and has a value of 1000 rev/min for the servo-pump to work with maximum efficiency; the necessary speed and torque can be provided by both a thermal engine or electric motor.

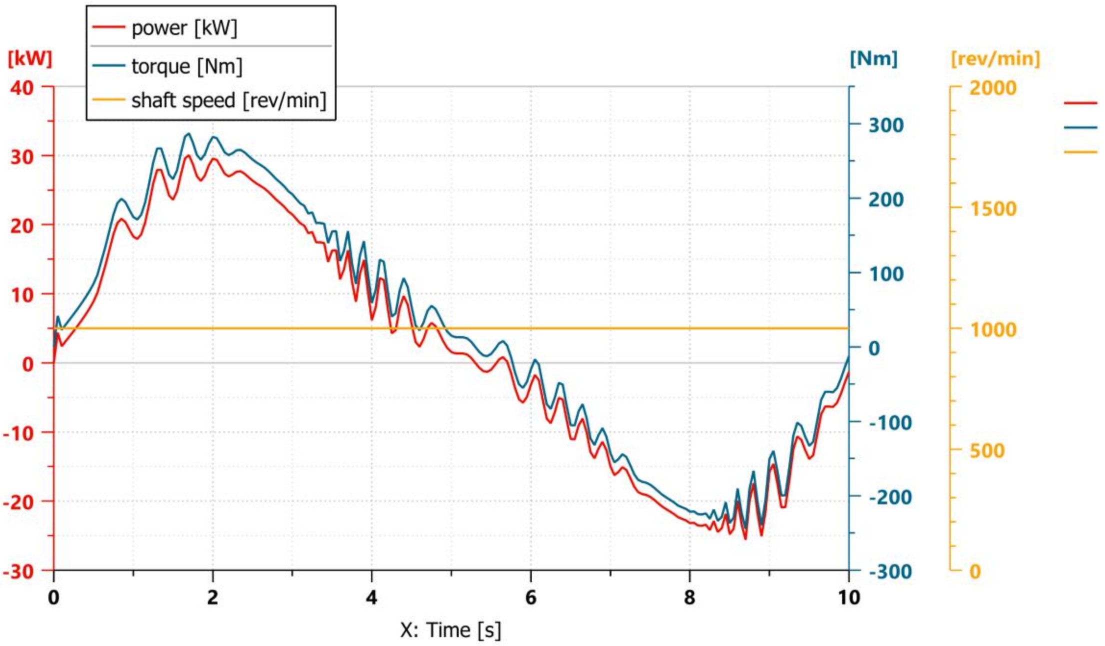

Fig. 4 - The speed, torque and power used by the servo-pump

The time-variation of the pressures on the two sides of the closed-loop hydrostatic transmission and the flow rate of the servo-pump are shown in Fig, 5; on this graph, one can see that the maximum pressure reached on one of the sides has the value of 170 bar, and on the other the pressure does not drop below the value of 20 bar, which means that cavitation does not occur on the pump suction port. The flow rate takes positive and negative values because it is measured at the same port and the sign shows the flow rate direction.

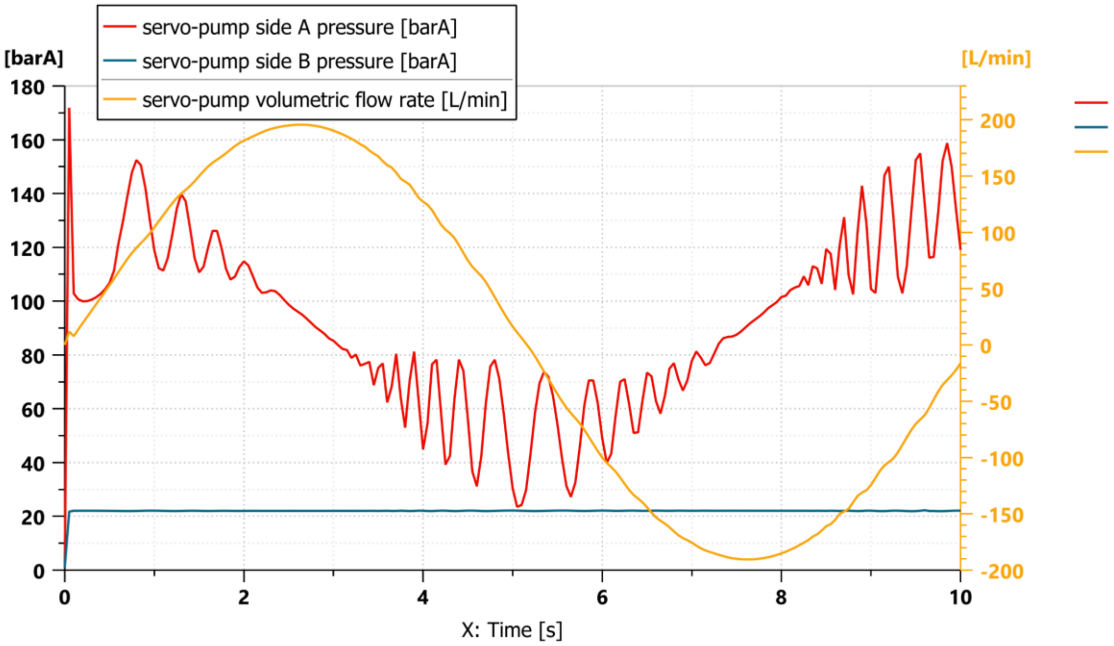

Fig. 5 - The pressures on the two sides of the closed-loop hydrostatic transmission and the flow rate of the servo pump

In the graph in Fig. 6, one can notice the variation over time of the various flow rates that pass through various components of the transmission; among them, the variation over time of the volumetric losses of the transmission can be noticed; those losses are proportional to the pressure in the system. Another curve of interest is that of the flow rate sent to the tank by the flush valve to be cooled and filtered and together with the volumetric losses, these two flow rates must have a value equal to that of the compensation pump that introduces cooled oil on the suction port of the main pump.

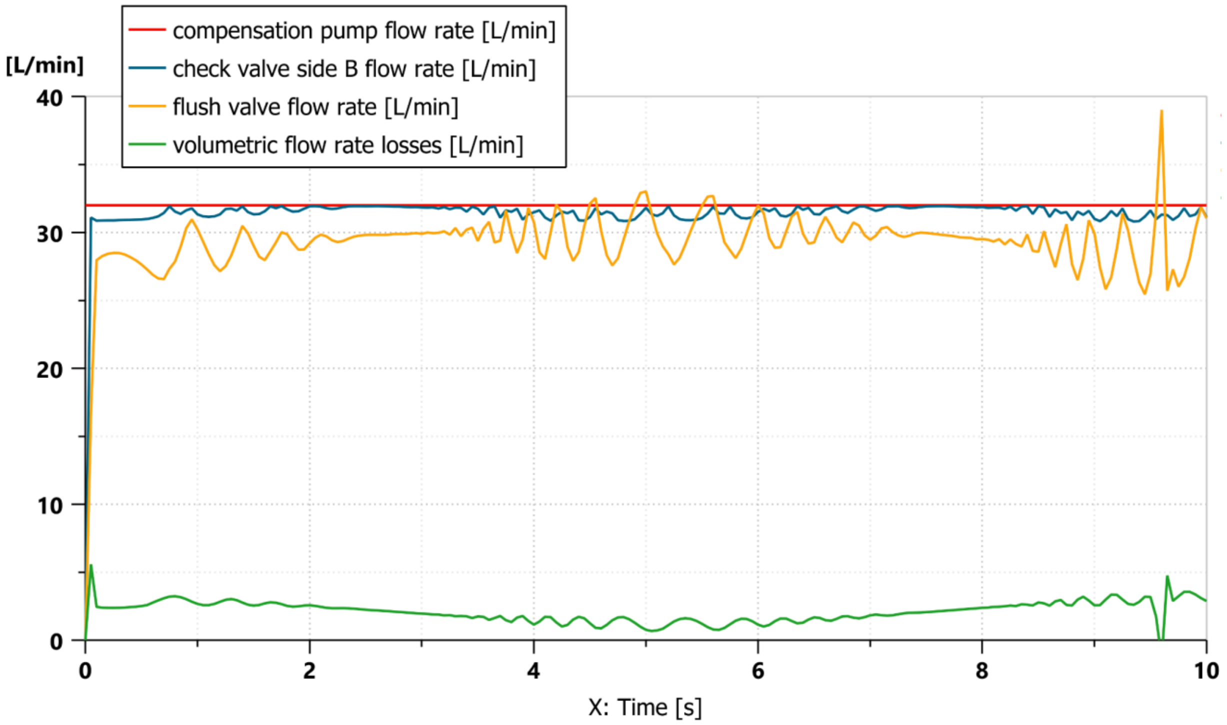

Fig. 6 - The flow rates through various components of the transmission and the amount of volumetric losses of the transmission

Fig. 7 shows the time-variation of hydraulic fluid parameters such as temperature, kinematic viscosity and undissolved gases.

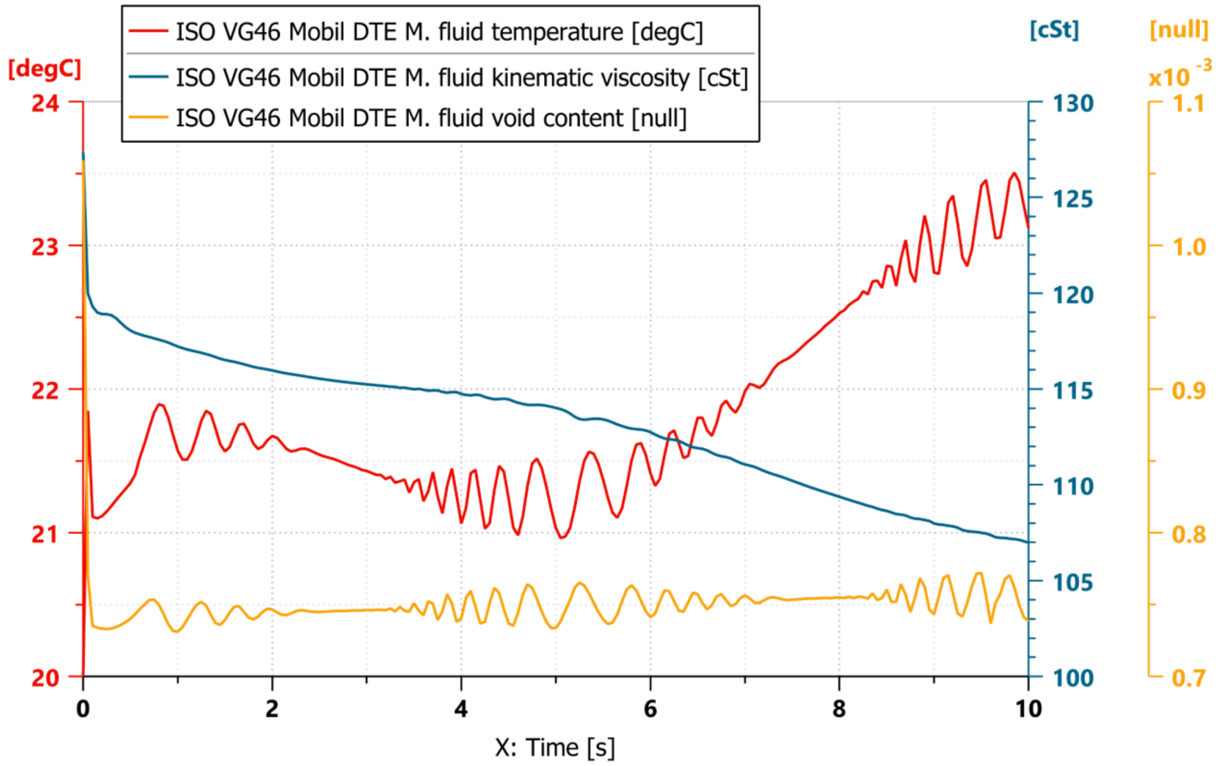

Fig. 7 - Hydraulic fluid parameters

In Fig. 8 one can see the time-variation of the flow rates and pressures at the ports of the two hydrostatic motors; in the same figure one can see how the flow divider divides the flow equally regardless of the pressure at the ports of the two hydrostatic motors.

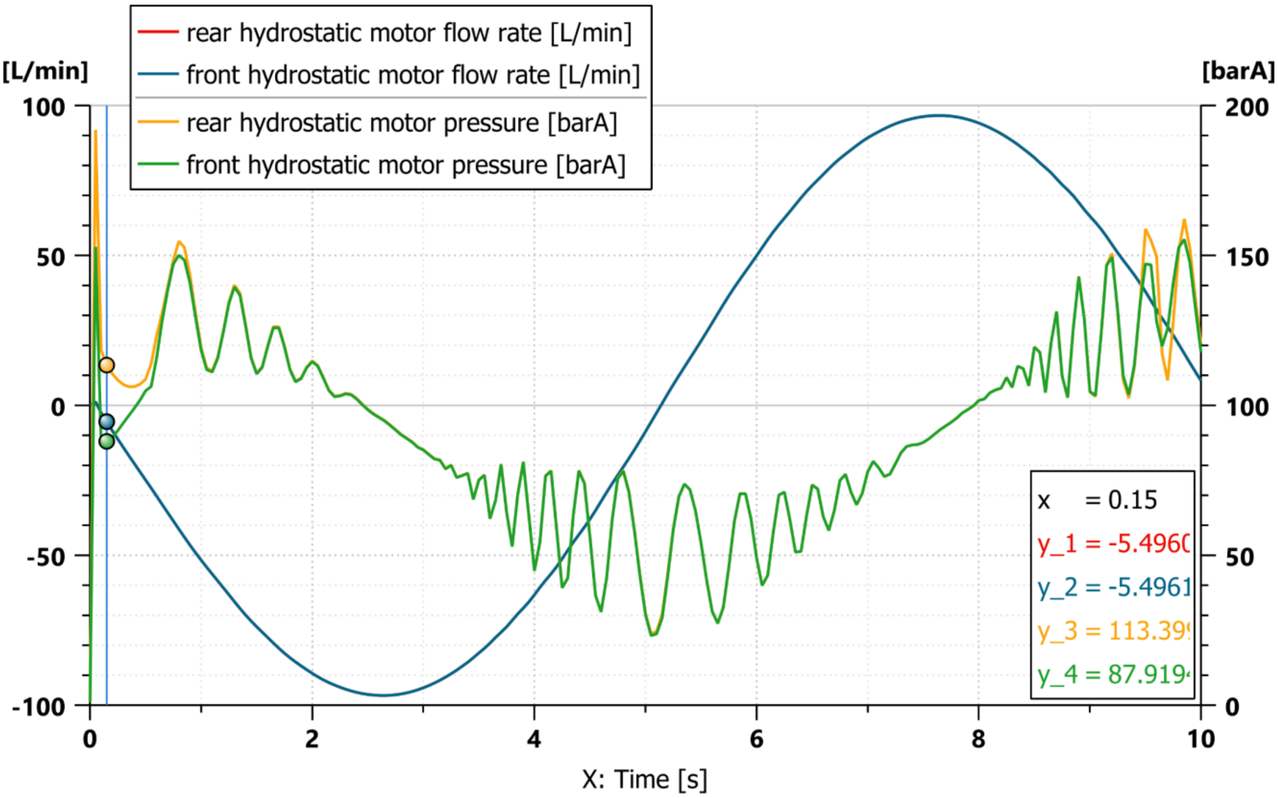

Fig. 8 – Flow rates and pressures at the ports of the two hydrostatic motors

The total mass of the platform and its payload, the slope of the ground as well as the variation over time of its profile can be seen in Fig. 9. On the same graph, it can be seen that the platform moves on rough terrain with unevenness of up to 0.025 m.

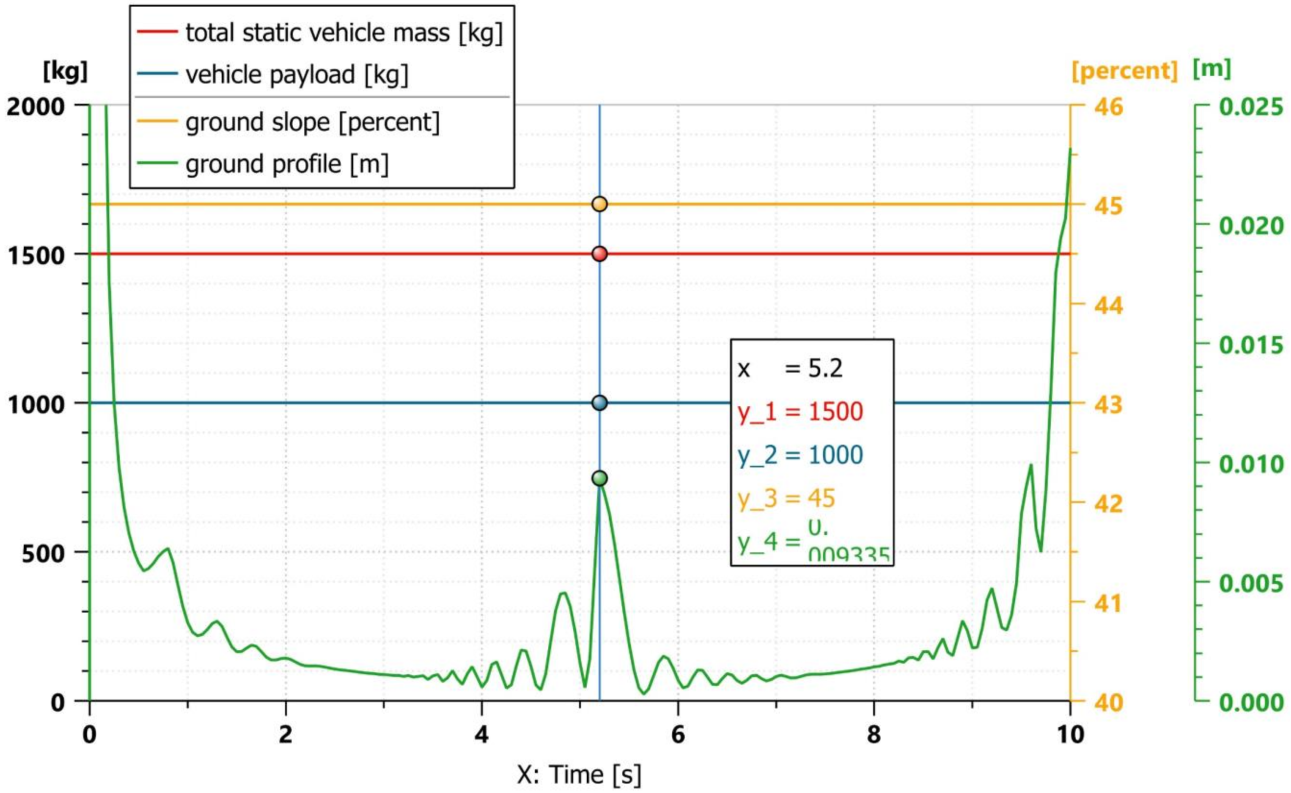

Fig. 9 – The total mass of the platform and its payload, the slope of the ground as well as its profile

The variation over time of the traction parameters of the agricultural platform are presented in Fig. 10; on this figure one can see how driving force is proportional to the acceleration of the platform.

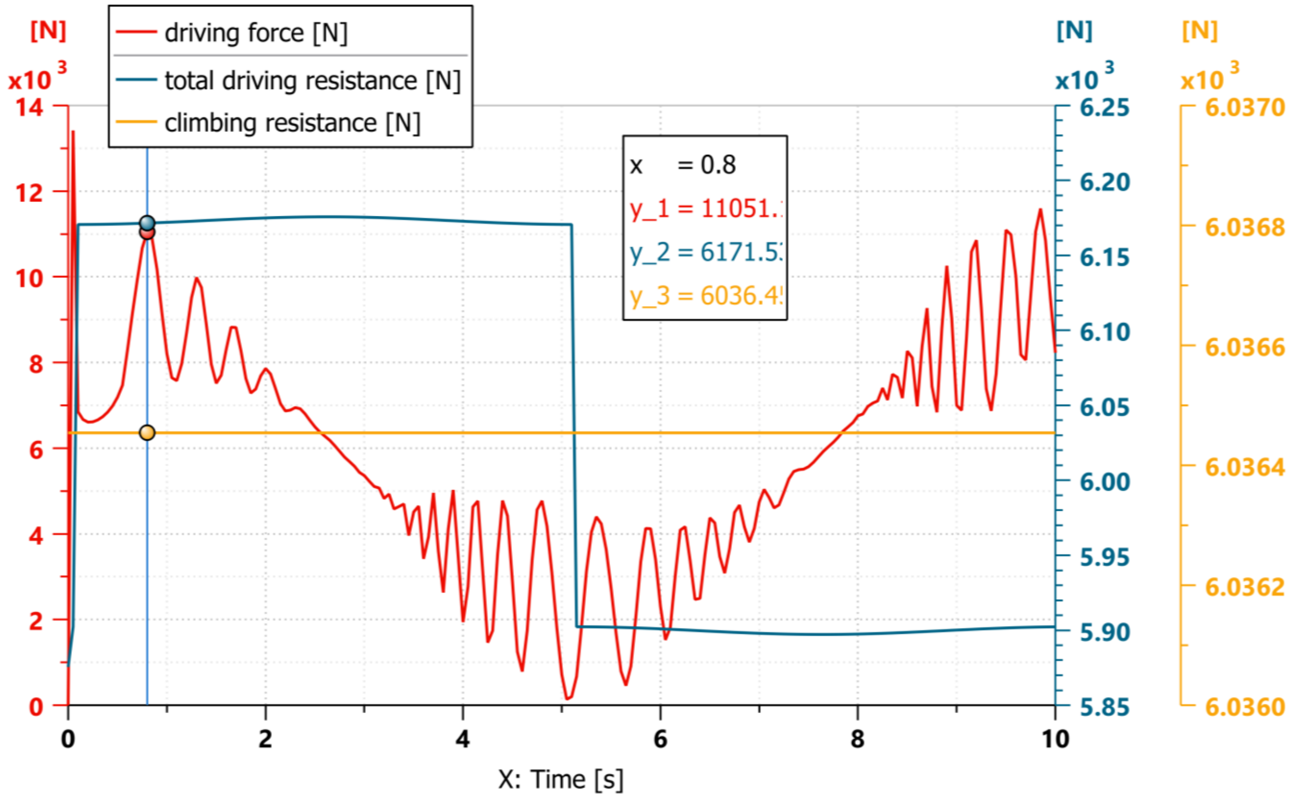

Fig. 10 – Driving force, total driving resistance and climbing resistance

Fig. 11 shows the torque variation over time of the wheels of the two driving axles, as well as their rotation speed, which is identical even if the torque of the two axles is different due to the uneven distribution of the mass of the platform on the two axles. The flow divider performs the role of a lockable differential.

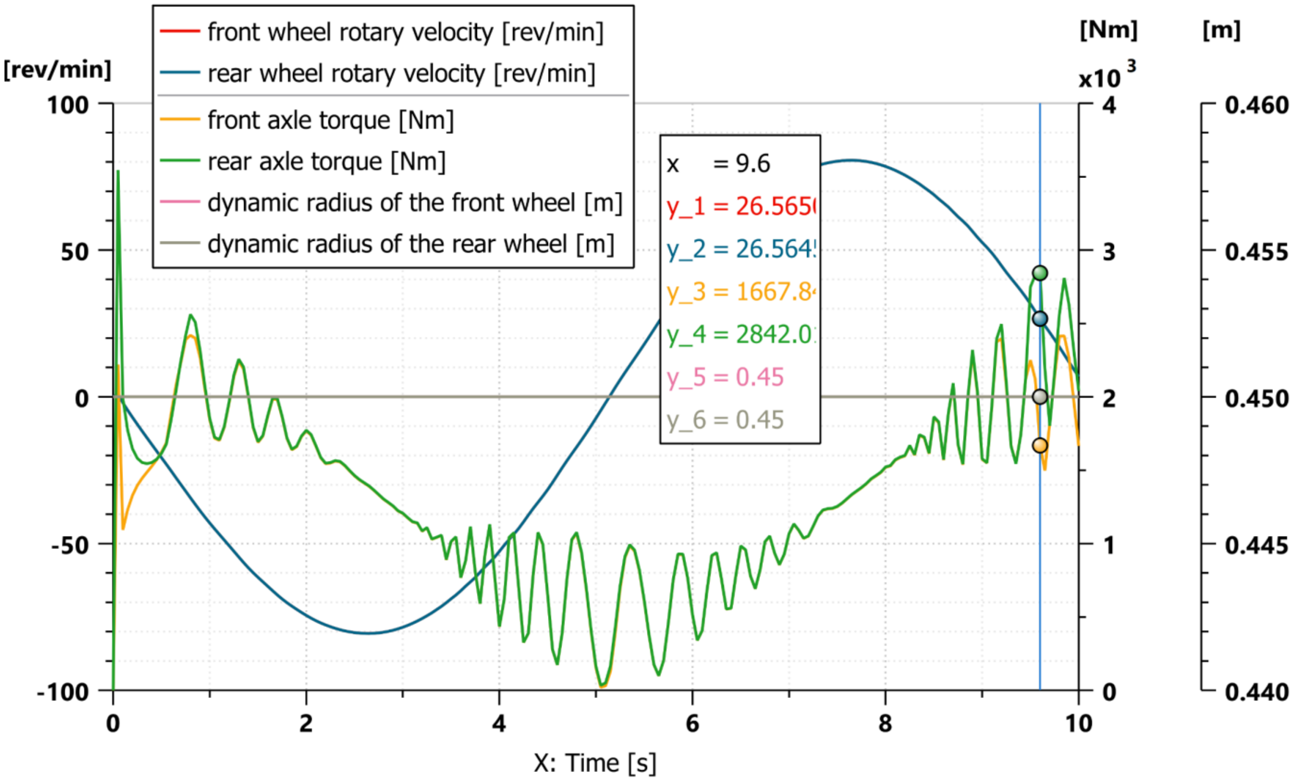

Fig. 11 – Platform wheels' velocity, torque and their dynamic radius

Fig. 12 shows the variation over time of the longitudinal slip expressed as a percentage of the driving axles of the agricultural platform; the values are different because the mass distribution on the two driving axles is different.

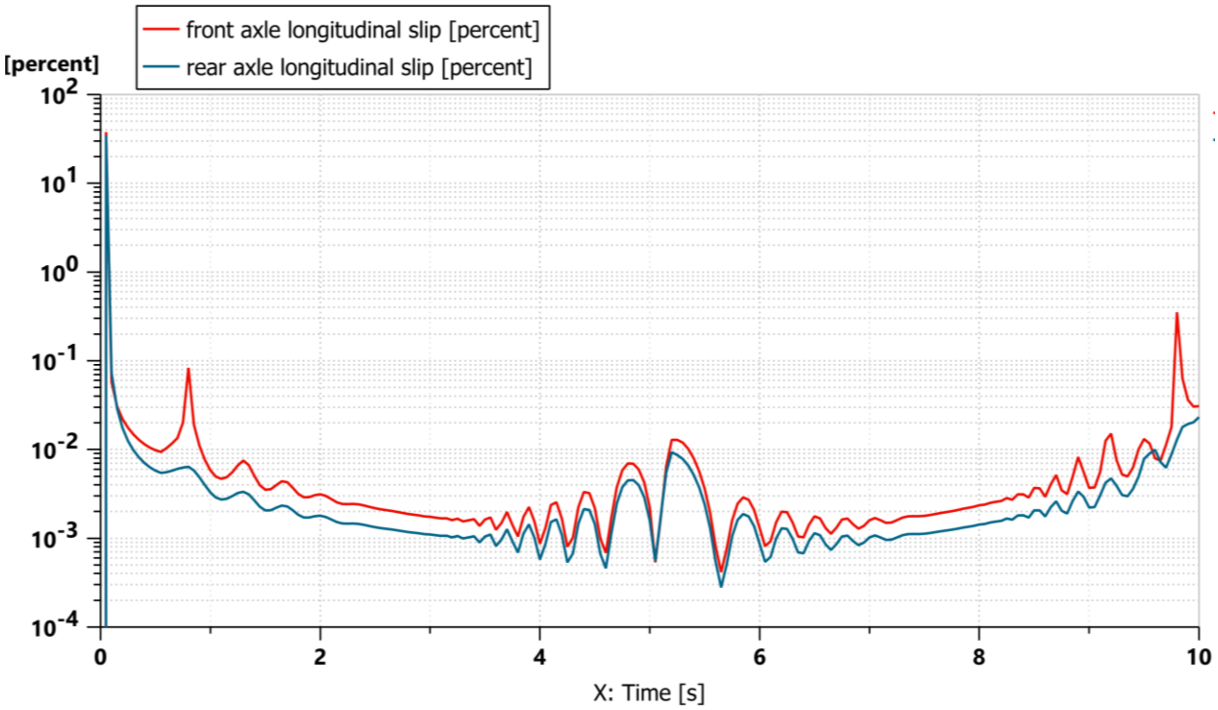

Fig. 12 – Longitudinal slip of the platform wheels (tires)

The time-variation of the dynamic parameters of the agricultural platform - linear displacement, linear velocity and linear acceleration - are presented in Fig. 13. On this figure, one can see the agricultural platform going up and down a slope, and reaching a certain altitude.

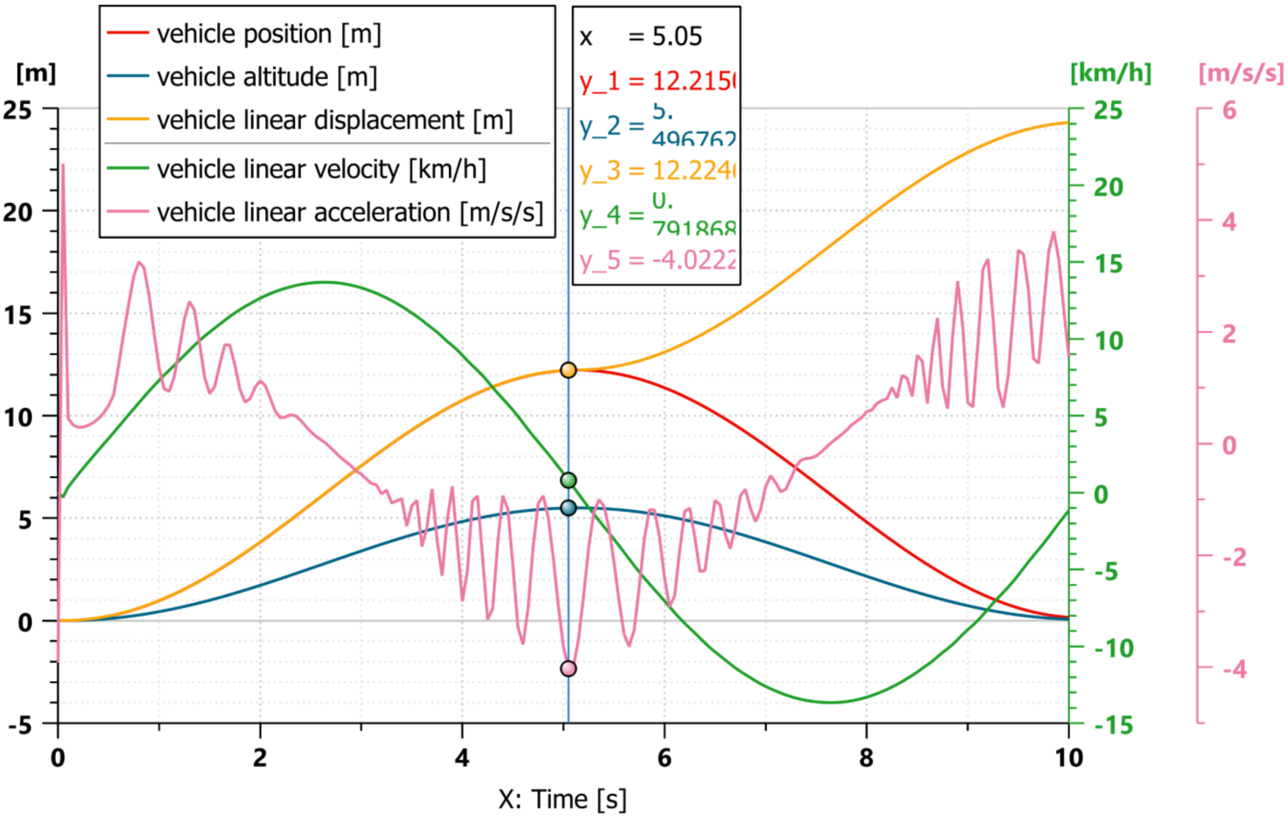

Fig. 13 - The dynamic parameters of the agricultural platform: linear displacement, linear velocity, linear acceleration and altitude

The time-variation of the control setpoint, plant value and instantaneous control error are shown in Fig. 14. In the same figure, it can be seen that the platform can achieve a continuously adjustable travel velocity of more than 12 km/h, which is the maximum velocity required for various technological works; the instantaneous adjustment error is small and is mainly due to the delay caused by the longitudinal slip of the wheels on the ground. It should be noted that the travel velocity is uniform and steady.

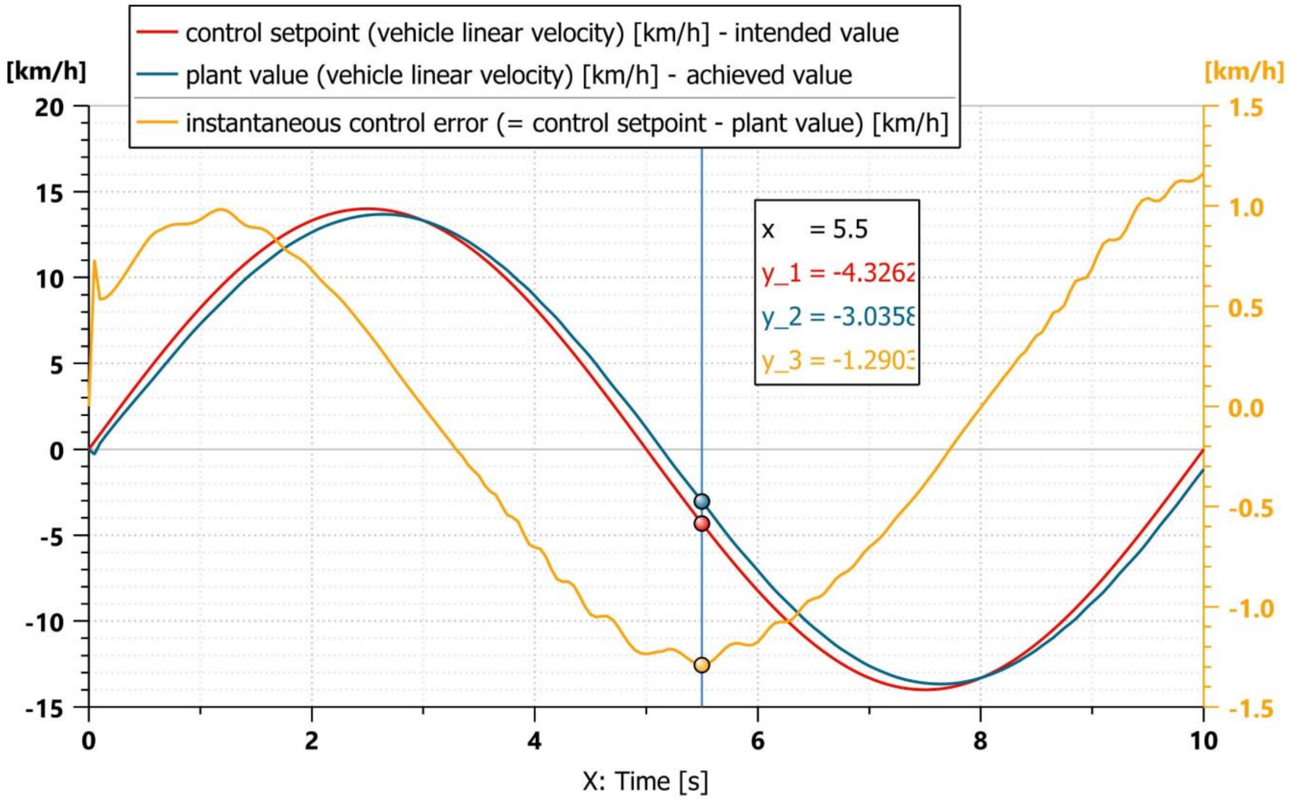

Fig. 14 - The performance of adjusting the travel speed of the agricultural platform

Since all the points in the graph in Fig. 15 are located to the left of the imaginary axis and in close proximity to the axis of real numbers or even on it, it follows that the system is stable and well damped.

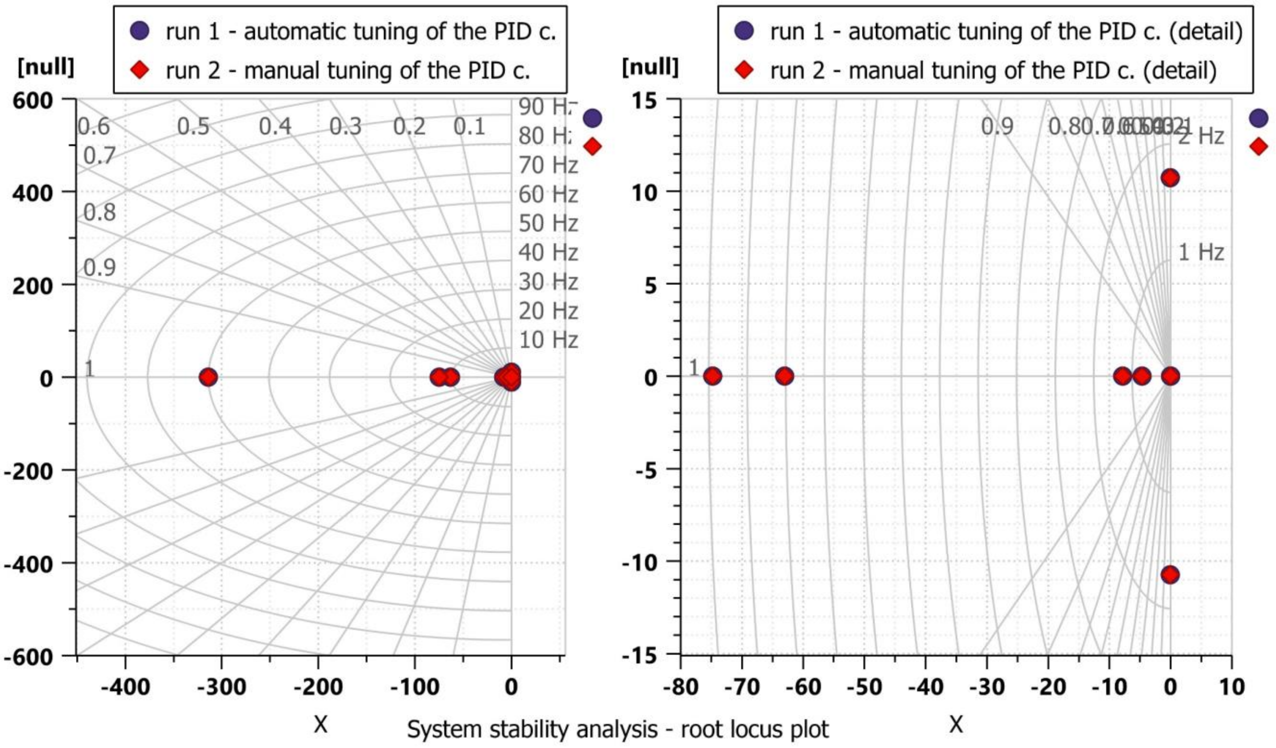

Fig. 15 - The plot of the stability analysis of the automatic adjustment system

CONCLUSIONS

The numerical simulation model is a scalable one and it can be used to study and optimize the dynamic parameters of closed-loop hydrostatic transmissions of various agricultural platforms.

Since the numerical simulation model is an advanced one that takes into account the influence of temperature on the hydraulic components, it can also be used for the precise sizing of the power required for the oil heat exchanger. The parameters of the hydraulic components in the simulation have been chosen in such a way that regardless of the operating conditions of the agricultural platform, it would work optimally in safe conditions.

Although the numerical simulation takes into account a terrain slope of 45%, for which the fluid pressure reaches max. 170 bar when the platform accelerates, the remaining pressure margin up to the nominal pressure of 300 bar would allow the platform to climb an even steeper slope or to tow heavy equipment.

Following the optimization of the dynamic parameters of the agricultural platform, one can notice that it is possible to achieve a continuous adjustment of the travel velocity, with a response time of max. 0.15 seconds, despite the non-linear disturbances of the physical process, which means that the platform can be used even for agricultural works that require high precision in velocity regulation and a fast response time.

ACKNOWLEDGEMENT

This paper has been financed under a project funded by the Ministry of Research, Innovation and Digitalization through Programme 1- Development of the national research & development system, Sub-programme 1.2 - Institutional performance - Projects financing the RDI excellence, Financial Agreement no. 18PFE/30.12.2021.

REFERENCES

[1] Balafoutis, A., Beck, B., Fountas, S., Tsiropoulos, Z., Vangeyte, J., van der Wal, T., Soto-Embodas, I., Gómez-Barbero, M., & and Pedersen, S. M., (2017), Smart Farming Technologies – Description, Taxonomy and Economic Impact, In: Pedersen, S., & Lind, K. (eds.) *Progress in Precision Agriculture*, Springer, Cham, ISBN 978-3-319-68713-1, pp. 21–77. https://doi.org/10.1007/978-3-319-68715-5_2;

[2] Cheng, Z., & Lu, Z., (2021), Research on Load Disturbance Based Variable Speed PID Control and a Novel Denoising Method Based Effect Evaluation of HST for Agricultural Machinery, *Agriculture*, vol. 11, no. 10, MDPI, ISSN 2077-0472, ID 960. https://doi.org/10.3390/agriculture11100960;

[3] Cheng, Z., & Lu, Z., (2022), Regression-Based Correction and I-PSO-Based Optimization of HMCVT's Speed Regulating Characteristics for Agricultural Machinery, *Agriculture*, vol. 12, no. 5, MDPI, ISSN 2077-0472, ID 580. https://doi.org/10.3390/agriculture12050580;

[4] Chiriță, Al.-P., & Pavel, C., (2022), Mathematical Modeling, Laboratory Testing and Numerical Simulation of a Servo-Pump as Part of a Closed Circuit Primary Control Hydrostatic Transmission for Multi-Purpose Trucks, *Hidraulica Magazine*, no. 4, Bucharest, ISSN 1453 – 7303, pp. 7-18;

[5] Guo, N., & Hu, J., (2014), Velocity Control System with Variable Universe Adaptive Fuzzy-PD Method for Agricultural Vehicles. *Proceeding of the 11th World Congress on Intelligent Control and Automation*, Shenyang / China, pp. 2148-2154. https://doi.org/10.1109/wcica.2014.7053054;

[6] Guo, N., Hu, J., & Wang, H., (2013), Intelligent operation control system for rice transplanter based on GPS navigation. *Nongye Jixie Xuebao/Transactions of the Chinese Society for Agricultural Machinery*, vol. 44, no. 1, ISSN 1000-1298, pp. 200-204. https://doi.org/10.6041/j.issn.1000-1298.2013.01.038;

[7] Hu, K., Zhang, W., Liu, H., & Li, K, (2021), Design and Simulation of the Hydraulic Driving System of Hilly Tractors, *Machine Tool & Hydraulics*, vol. 49, no. 16, ISSN 1001-3881, pp. 93–97. https://doi.org/10.3969/j.issn.1001-3881.2021.16.019;

[8] Li, J., Li, S., Zhang, Y., Wu, H., Liu, M., & Gao, Z., (2021), Design of hydraulic drive system for mountain orchard transporter, *J. Anhui Agric. Univ.*, vol. 48, no. 1, ISSN 1672-352X, pp. 143–149;

[9] Tecușan, N., & Ionescu, E., (1982), *Tractors and automobiles (Tractoare și automobile)*. Bucharest/Romania, Didactic and Pedagogical Publishing House;

[10] Warring, R. H., (2014), *Some Aspects of Hydraulics in Mechanical Handling and Mobile Equipment*. Morden, Elsevier, ISBN 9781483296104;

[11] Zhang, Q. (ed.), (2015), *Precision Agriculture Technology for Crop Farming*. Boca Raton, CRC Press, ISBN 9781482251081.